学位論文

Subtyping of non-small cell lung carcinoma into adenocarcinoma and squamous cell carcinoma by cytological structural features

香川大学大学院医学系研究科

医学専攻

井上耕佑

Research Article

Subtyping of Non-small Cell Lung Carcinoma into Adenocarcinoma and Squamous Cell Carcinoma by Cytological Structural Features

Kosuke Inoue[a], Reiji Haba[b], Kana Kiyonaga[b], Toru Matsunaga [b], Seiko Kagawa [b], Toshitetsu Hayashi[c], Ryou Ishikawa[b]

[a] Department of Diagnostic Pathology, Sumitomo Besshi-Hospital, Ehime, Japan

[b] Department of Diagnostic Pathology, Kagawa University Hospital, Kagawa, Japan

[c] Department of Diagnostic Pathology and Cytology, Kuma Hospital, Hyogo, Japan

Short Title: SUBTYPING OF NON-SMALL CELL LUNG CARCINOMA BY CYTOLOGICAL STRUCTURAL FEATURES

Corresponding Author:

Kosuke Inoue

Department of Diagnostic Pathology

Sumitomo Besshi Hospital

3-1 Oji-Cho

Niihama City, Ehime Prefecture, 792-8543, Japan

Tel: +818031680900

E-mail: kosuke_inoue@ni.sbh.gr.jp

Number of Tables: 1

Number of Figures: 14

Word count: 3188

Keywords: Cytology, Non-small cell lung carcinoma, Cytological structural features, Adenocarcinoma, Squamous cell carcinoma

Abstract

Introduction: This study aimed to clarify the diagnostic structural features in cytology specimens that are useful in subtyping non-small cell lung carcinoma (NSCLC) into adenocarcinoma (ADC) and squamous cell carcinoma (SQCC).

Methods: Cytology specimens (n = 233) of NSCLCs, which included ADCs (n = 149) and SQCCs (n = 84), were analyzed. The following cytological features were evaluated: isolated cell, flat sheet, three-dimensional cluster with irregular arrangement, papillary-like structure, micropapillary-like structure, acinar-like structure, palisading pattern, protrusion of nuclei at the periphery of the cluster, honeycomb pattern, streaming arrangement, three-dimensional sheets with regular arrangement, flattening at the periphery of the cluster, fuzzy pattern at the periphery of the cluster, and mutual inclusion.

Results: ADCs exhibited significantly higher frequencies of flat sheet ($p < 0.001$), papillary-like structure ($p < 0.001$), micropapillary-like structure ($p = 0.028$), acinar-like structure ($p < 0.001$) and protrusion of nuclei at the periphery of the cluster ($p < 0.001$) than SQCCs. The latter exhibited significantly higher frequencies of streaming arrangement ($p < 0.001$), three-dimensional sheets with regular arrangement ($p < 0.001$), flattening at the periphery of the cluster ($p < 0.001$), fuzzy pattern at the periphery of the cluster ($p < 0.001$), and mutual inclusion ($p < 0.001$) than ADCs.

Discussion/Conclusion: Cytological structural features, such as flat sheet, papillary-like structure, micropapillary-like structure, acinar-like structure, and protrusion of nuclei at the periphery of the cluster, indicated ADC, whereas streaming arrangement, three-dimensional sheets with regular arrangement, flattening at the periphery of the cluster, fuzzy pattern at the periphery of the cluster, and mutual inclusion indicated SQCC. Paying attention to these cytological structural features can enable the accurate subtyping of NSCLC into ADC and SQCC.

Introduction

Lung cancer is the most common cause of cancer death worldwide [1]. Distinguishing non-small cell lung carcinoma (NSCLC) from small cell carcinoma is important for deciding the therapeutic strategy. With the development of target-specific therapies, the importance of subtyping NSCLC into adenocarcinoma (ADC) and squamous cell carcinoma (SQCC) has been increasingly realized in order to decide the therapeutic strategy. For ADC, testing of epidermal growth factor receptor (EGFR) mutation and anaplastic lymphoma kinase (ALK) and ROS proto-oncogene 1 (ROS1) fusion is important [2]. For SQCC, bevacizumab administration is contraindicated owing to the risk of life-threatening hemoptysis [3]. The combination of pemetrexed and cisplatin has shown worse overall survival in patients with SQCC than in those with other NSCLC [4].

Approximately 70% of lung carcinomas are unresectable because patients present with advanced-stage disease [5]; small biopsy and cytology specimens are the primary diagnostic tools for the majority of patients with lung carcinoma. Thus, correct subtyping of NSCLC into ADC and SQCC would be important for cytology specimens. Subtyping of NSCLC into ADC and SQCC in small biopsy and cytology specimens has been recommended [6-8]. Although ancillary techniques such as immunohistochemistry (IHC), are useful for distinguishing histological types of NSCLC, it is preferable to minimize IHC and use morphological analysis alone for diagnosis considering that specimens may be spared for molecular testing (e.g., EGFR) [5] [8].

Subtyping of NSCLC in cytology specimens is mainly based on cytological features. For instance, foamy cytoplasm, eccentrically situated nuclei, granular chromatin, and single prominent nucleolus indicate ADC [9]. Keratinization, dense cytoplasm, centrally situated nuclei, coarse granular chromatin, and multiple nucleoli indicate SQCC [9].

Recently, development of techniques for collecting specimens, such as in bronchoscopy biopsy and fine needle aspiration cytology, has led to increased proportion of fresh specimens. In fresh cytology specimens, structural features can be observed more precisely, and evaluation of the structural features can contribute remarkably to the determination of histologic subtypes. In the 8th edition of General Rule for Clinical and Pathological Record of Lung Cancer (Japanese classification of lung carcinoma), some structural features of cytology specimens that were potential clues for subtyping NSCLC into ADC and SQCC were proposed [9]. We selected 14 cytological features therefrom and evaluated them to clarify the diagnostic structural features in cytology specimens. To the best of our knowledge, this is the first study that aimed to revalidate the diagnostic value of the 14 cytologic structural features.

This study aimed to clarify the diagnostic structural features in cytology specimens that help in subtyping NSCLC into ADC and SQCC.

Materials and Methods

Patients and study design

This study was conducted in the Department of Diagnostic Pathology, Kagawa University Hospital (Takamatsu City, Kagawa Prefecture, Japan). Cytology specimens of primary lung ADC or SQCC, diagnosed over a 4-year period (January 2017 to December 2020), were retrospectively evaluated.

The cytology specimens included exfoliative and fine needle aspiration (FNA). Cases with a paired concomitant or subsequent histologic diagnosis as ADC or SQCC using biopsies or surgical specimens were eligible for this study. Histological diagnosis was based on morphological analysis or IHC. Morphologically, cases showing glandular structure or intracytoplasmic mucin were classified as ADC, while those showing keratinization or intercellular bridge were classified as SQCC. For those that did not show any of the above morphological features, immunohistochemical staining for TTF-1 and p40 was performed, and those that were TTF-1-positive were classified as ADC and those that were p40-positive were classified as SQCC (shown in Fig. 1). Metastatic tumors were excluded. The specimens were fixed with 95% ethanol and stained using the Papanicolaou method.

Evaluation of cytological structural features

Cytology specimens were examined by two pathologists and a cytotechnologist. They were evaluated based on the presence or absence of each cytological structural feature; isolated cell, flat sheet, three-dimensional cluster with irregular arrangement, papillary-like structure, micropapillary-like structure, acinar-like structure, palisading pattern, protrusion of nuclei at the periphery of the cluster, honeycomb pattern, streaming arrangement, three-dimensional sheets with regular arrangement, flattening at the periphery of the cluster, fuzzy pattern at the periphery of the cluster, and mutual inclusion. Discrepant interpretations across the evaluators were resolved by consensus.

Statistical analysis

Statistical analyses were performed with SPSS software (IBM Japan, Chuo City, Tokyo Capital, Japan). Sensitivity, specificity, positive predictive value, and negative predictive value were calculated for each structural feature. Pearson's chi-squared test or Fisher's exact test was applied to verify the association between each cytological structural feature and histological subtype. The level of statistical significance was set at $p < 0.05$.

Results

A total of 233 cases were included in the analysis; of them, 149 were ADC (63.9%) and 84 were SQCC (36.1%). The cytological findings are summarized in Table 1.

Flat sheet, papillary-like structure, micropapillary-like structure, acinar-like structure, and protrusion of nuclei at the periphery of the cluster were detected at a significant frequency in ADC. Streaming arrangement, three-dimensional sheets with regular arrangement, flattening at the periphery of the cluster, fuzzy pattern at the periphery of the cluster, and mutual inclusion were detected at a significant frequency in SQCC.

1 Isolated cell

The tumor cells were poorly cohesive and singly scattered (shown in Fig. 2). There were 137 ADCs and 78 SQCCs; the sensitivity, specificity, positive predictive value, and negative predictive value for ADC were 91.9%, 7.1%, 63.7%, and 33.3%, respectively. There was no statistically significant difference (p value = 0.803).

2 Flat sheet

The cluster was composed of flat mono-layered tumor cells. The cluster with well-defined cell borders was classified as honeycomb pattern (shown in Fig. 3). There were 42 ADCs and 5 SQCCs; the sensitivity, specificity, positive predictive value, and negative predictive value for ADC were 28.2%, 94.0%, 89.4%, and 42.5%, respectively. The difference between ADC and SQCC was statistically significant (p value < 0.001).

3 Three-dimensional cluster with irregular arrangement

The cluster was composed of more than three tumor cell layers. Arrangement of the tumor cells was irregular (shown in Fig. 4). There were 137 ADCs and 76 SQCCs; the sensitivity, specificity, positive predictive value, and negative predictive value for ADC were 91.9%, 9.5%, 64.3%, and 40.0%, respectively. There was no statistically significant difference (p value = 0.701).

4 Papillary-like structure

The cluster was composed of medium to large numbers of tumor cells. Peripheral tumor cells of the cluster protruded outward in peninsula shape with or without a fibrovascular core (shown in Fig.5). There were 64 ADCs and 11 SQCCs; the sensitivity, specificity, positive predictive value, and negative predictive value for ADC were 43.0%, 86.9%, 85.3%, and 46.2%, respectively. The difference between ADC and SQCC was statistically significant (p value < 0.001).

5 Micropapillary-like structure

The clusters were composed of 3–20 tumor cells with flower crown-like, ball-like, or mulberry-like formation (shown in Fig. 6). There were nine ADCs and no SQCCs; the sensitivity, specificity, positive predictive value and, negative predictive value for ADC were 6.0%, 100.0%, 100.0%, and 37.5%, respectively. The difference between ADC and SQCC was statistically significant (p value = 0.028).

6 Acinar-like structure

The cluster showed circular arrangements of tumor cells with lacunae. Arrangements without lacuna were excluded (shown in Fig. 7). There were 52 ADCs and 5 SQCCs; the sensitivity, specificity, positive predictive value, and negative predictive value for ADC were 35.1%, 94.0%, 91.2%, and 45.1%, respectively. The difference between ADC and SQCC was statistically significant (p value < 0.001).

7 Palisading pattern

Columnar tumor cells showed palisading arrangement at the periphery of the cluster (shown in Fig. 8). There were four ADCs and one SQCCs; the sensitivity, specificity, positive predictive value, and negative predictive value for ADC were 2.7%, 80.0%, 98.8%, and 36.4%, respectively. There was no statistically significant difference (p value = 0.656).

8 Protrusion of nuclei at the periphery of the cluster

Nuclei at the periphery of the cluster protruded outwards. The length of the protruding nuclei was more than half the length of the nuclei. Two or more nuclei of tumor cells were required for the protrusion (shown in Fig. 9). There were 122 ADCs and 35 SQCCs; the sensitivity, specificity, positive

predictive value, and negative predictive value for ADC were 81.9%, 58.3%, 77.7%, and 64.5%, respectively. The difference between ADC and SQCC was statistically significant (p value < 0.001).

9 Honeycomb pattern

The cluster was composed of flat mono-layered tumor cells with sharply delineated cell borders. Nuclei of the tumor cells were located in the center of the cytoplasm (shown in Fig. 10). There were two ADCs and no SQCCs; the sensitivity, specificity, positive predictive value, and negative predictive value for ADC were 1.3%, 100.0%, 100.0%, and 36.4%, respectively. There was no statistically significant difference (p value = 0.537).

10 Streaming arrangement

The tumor cells with oval or spindle nuclei showed fascicular structure along the direction of major axis of the nuclei in the cluster (shown in Fig. 11). There were 11 ADCs and 47 SQCCs; the sensitivity, specificity, positive predictive value and negative predictive value for SQCC were 56.0%, 92.6%, 81.0%, and 78.9%, respectively. The difference between ADC and SQCC was statistically significant (p value < 0.001).

11 Three-dimensional sheets with regular arrangement

The cluster was composed of layered sheets of tumor cells with evenly distributed nuclei (shown in Fig. 12). There were three ADCs and 34 SQCCs; the sensitivity, specificity, positive predictive value and negative predictive for SQCC value were 40.5%, 98.0%, 91.9%, and 74.5%, respectively. The difference between ADC and SQCC was statistically significant (p value < 0.001).

12 Flattening at the periphery of the cluster Nuclei of tumor cells located in the periphery of the cluster were elongated and flat (shown in Fig. 10). There were 17 ADCs and 50 SQCCs; the sensitivity, specificity, positive predictive value, and negative predictive value for SQCC were 59.5%, 88.6%, 74.6%, and 79.5%, respectively. The difference between ADC and SQCC was statistically significant (p value < 0.001).

13 Fuzzy pattern at the periphery of the cluster

Cytoplasmic elongation of tumor cells was seen toward the outside of the cluster. Two or more cytoplasmic elongations were needed (shown in Fig. 13). There were 12 ADCs and four SQCCs; the sensitivity, specificity, positive predictive value, and negative predictive value for SQCC were 28.6%, 91.9%, 66.7%, and 69.5%, respectively. The difference between ADC and SQCC was statistically significant (p value < 0.001).

14 Mutual inclusion

Two tumor cells showed a structure that appeared like a single cell englobing another cell (shown in Fig. 14). There were 38 ADCs and 61 SQCCs; the sensitivity, specificity, positive predictive value, and negative predictive value for SQCC were 72.6%, 74.5%, 61.6%, and 82.8%, respectively. The difference between ADC and SQCC was statistically significant (p value < 0.001).

Discussion/Conclusion

Previously, there were no therapeutic implications for further classification of NSCLC; hence, very little attention was given to the distinction of ADC from SQCC in small tissue samples [5]. Recently, with the development of target-specific therapies, the need for accurate subtyping of non-small cell carcinoma into ADC and SQCC has arisen for appropriate clinical decision making. Most lung carcinomas are diagnosed in advanced unresectable stage, and the diagnosis is often done exclusively from cytology or small biopsy specimens [5]. Although typing of NSCLC into ADC and SQCC is often recommended in small biopsy and cytology specimens [6-8], differentiating between ADC and SQCC is sometimes challenging in cytology specimens.

The accuracy of subtyping NSCLC into ADC and SQCC in cytology specimens has been reported previously. Rekhtman et al. had reported that accuracy of cytological tumor subtyping in concordance with histologic diagnosis was 96% in ADC and SQCC cases [10]. Edward et al. had reported that comparison of preoperative tumor classification of cytology specimens with postoperative classification showed the rate of correct specific preoperative diagnosis to be 32% in ADC and 64% in SQCC [11]. Nizzoli et al. reported both cytological and histological typing to be concordant in 88% of ADC and SQCC cases [12]. Although accurate tumor subtyping may not always be obtained by cytology specimen only, as mentioned above, subtyping of NSCLC into ADC and SQCC should be done whenever possible.

In recent years, the frequency of fresh cytology specimens has increased due to the development of techniques of specimen collection, such as in bronchoscopy biopsy and fine needle aspiration cytology. In fresh cytology specimens, structural features can be observed more precisely.

In a previous report, some cytological structural features that were clues to subclassify NSCLC into ADC and SQCC had been mentioned. Jhonston et al. had reported acinar structure in cytology specimens of ADC [13]. Nandeesh et al. had reported that glands and three-dimensional and papillary clusters are seen in ADC while single cells are seen in SQCC [14]. MacDonald et al. previously reported that the mono-layered sheet is a feature that indicated bronchioloalveolar carcinoma, corresponding to adenocarcinoma in situ in the 2021 World Health Organization classification of lung tumors [15]. Morency et al. had reported a drunken honeycomb pattern in invasive mucinous adenocarcinoma [16]. Idowu et al. enumerated the cytomorphological features of adenocarcinoma, including three-dimensional clusters, individual cells, acinar arrangements, or papillary fronds with fibrovascular septa. They also reported that well-differentiated SQCC typically appears as individual cells or cohesive sheets of tumor cells [17].

In the current study, the presence of cytological structural features, such as flat sheet, papillary-like structure, micropapillary-like structure, acinar-like structure, or protrusion of nuclei at the periphery of the cluster, provided clues that indicated ADC. Flat sheet would correspond to lepidic pattern of growth in adenocarcinoma in situ, minimally invasive adenocarcinoma, or lepidic adenocarcinoma. This cytological structural feature was seen in a small number of ADC cases, such as acinar adenocarcinoma, papillary adenocarcinoma, micropapillary adenocarcinoma, or solid adenocarcinoma cases; it was seldom seen in SQCC cases. Papillary-like structures were seen in ADC cases with papillary pattern of growth. This cytological structural feature was also seldom seen in SQCC cases. Micropapillary-like structure was observed in ADC cases with micropapillary pattern of

growth. No SQCC case showed micropapillary-like structure. Acinar-like structure was seen in ADC cases with acinar or cribriform structure pattern of growth; it was seldom seen in SQCC cases. Protrusion of nuclei at the periphery of the cluster was seen in ADC with any architectural pattern; it was also observed in some SQCC cases.

Presence of cytological structural features, such as streaming arrangement, three-dimensional sheets with regular arrangement, flattening at the periphery of cluster, fuzzy pattern at the periphery of the cluster, or mutual inclusion, provided clues that indicated SQCC. Streaming arrangement, three-dimensional sheets with regular arrangement, and flattening at the periphery of the cluster were observed in poorly differentiated SQCC cases, such as non-keratinizing squamous cell carcinoma or basaloid squamous cell carcinoma; therefore, these structural features could play an important role in the diagnosis of SQCC cases having no keratinization in cytology specimen. It was noteworthy that mutual inclusion could be seen in not only SQCC cases but also ADC cases.

In this study, palisading pattern and honeycomb pattern had no statistical significance, although they had high specificity and positive predictive value. A palisading pattern was observed in papillary adenocarcinoma, invasive mucinous adenocarcinoma, and basaloid squamous cell carcinoma cases; it could also be seen in enteric adenocarcinoma, fetal adenocarcinoma or metastatic colonic carcinoma. A honeycomb pattern was observed in invasive mucinous adenocarcinoma cases, in this study; it could also be seen in fetal adenocarcinoma.

Although the cytological structural features, with statistically significant difference, would be characteristic of ADC or SQCC, a single cytological parameter is usually less reliable as a specific feature of ADC or SQCC. In this study, although flat sheet and acinar-like structures had high specificity and positive predictive value for ADC, the structural features were seen in some SQCC cases as well. Although three-dimensional sheets with regular arrangement had high specificity and positive predictive value for SQCC, the features were seen in some ADC cases as well. Nizzoli et al. had reported an SQCC case in which acinar-like structure was seen [12]. When two or more of these cytological structural features are present in combination, the diagnostic accuracy would be high.

A limitation of this study is that some cytologic structural features were relatively small in number, such as micropapillary-like structure, palisading pattern, and honeycomb pattern. A study with a large number of NSCLC cases would be required in the future. Another limitation is that the cytologic structural features could possibly have diagnostic discrepancies.

In conclusion, we evaluated the diagnostic value of cytological structural features in cytology specimens to obtain more accurate subtyping of NSCLC into ADC and SQCC. To the best of our knowledge, this is the first study to focus on the structural features of cytology specimen of NSCLC and revalidate the diagnostic value of cytological structural features described in the General Rule for Clinical and Pathological Record of Lung Cancer (the 8th edition). The cytological structural features would overall help to make accurate diagnosis of NSCLC.

Statement of Ethics

The study protocol was approved by the Ethics Committee of Kagawa University Hospital (approval number: 2021-015; approval date: May 14, 2021). Written informed consent was waived for this retrospective study by the Ethics Committee of Kagawa University Hospital.

Conflict of Interest Statement

The authors have no conflicts of interest to declare.

Funding Sources

The authors received no specific funding for this project.

Author Contributions

Inoue K., Haba R., and Kiyonaga K. contributed to the study concept and design, and reviewed the glass slides. Haba R., Kiyonaga K., Matsunaga T., Kagawa S., Hayashi T., and Ishikawa R. critically revised the manuscript.

Data Availability Statement

All data generated or analyzed during this study are included in this article. Further inquiries can be directed to the corresponding author.

References

1 Sung H, Ferlay J, Siegel RL, Laversanne M, Soerjomataram I, Jemal A, et al. Global cancer statistics 2020: GLOBOCAN estimates of incidence and mortality worldwide for 36 cancers in 185 countries. CA Cancer J Clin. 2021 May;71(3):209–49.

2 Lindeman NI, Cagle PT, Aisner DL, Arcila ME, Beasley MB, Bernicker EH, et al. Updated molecular testing guideline for the selection of lung cancer patients for treatment with targeted tyrosine kinase inhibitors: guideline from the College of American Pathologists, the International Association for the Study of Lung Cancer, and the Association for Molecular Pathology. Arch Pathol Lab Med. 2018 Mar;142(3):321–46.

3 Johnson DH, Fehrenbacher L, Novotny WF, Herbst RS, Nemunaitis JJ, Jablons DM, et al. Randomized phase II trial comparing bevacizumab plus carboplatin and paclitaxel with carboplatin and paclitaxel alone in previously untreated locally advanced or metastatic non-small-cell lung cancer. J Clin Oncol. 2004 Jun 1;22(11):2184–91.

4 Selvaggi G, Scagliotti GV. Histologic subtype in NSCLC: does it matter? Oncology (Williston Park). 2009 Nov 30;23(13):1133–40.

5 Travis WD, Brambilla E, Noguchi M, Nicholson AG, Geisinger K, Yatabe Y, et al. Diagnosis of lung cancer in small biopsies and cytology: implications of the 2011 International Association for the Study of Lung Cancer/American Thoracic Society/European Respiratory Society classification. Arch Pathol Lab Med. 2013 May;137(5):668–84.

6 Travis WD, Brambilla E, Noguchi M, Nicholson AG, Geisinger KR, Yatabe Y, et al. International Association for the Study of Lung Cancer/American Thoracic Society/European Respiratory Society international multidisciplinary classification of lung adenocarcinoma. J Thorac Oncol. 2011 Feb;6(2):244–85.

7 Travis WD, Brambilla E, Burke AP, Marx A, Andrew G. Nicholson. WHO classification of tumours of the lung, pleura, Thymus and heart. 4th ed. Lyon France: International Agency for Research on Cancer; 2015.

8 Editorial Board. Thoracic Tumors. WHO Classification of Tumours. World Health Organ Classif Tumours. 5th ed. Lyon France: International Agency for Research on Cancer. 2021.

9 Yushima BK, To T. The Japan lung cancer society. General Rule for clinical and pathological record of lung cancer. 8th ed 2-31-14. Japan: Kanehara Shuppan; 2017. Vols. 113–0034.

10 Rekhtman N, Brandt SM, Sigel CS, Friedlander MA, Riely GJ, Travis WD, et al. Suitability of thoracic cytology for new therapeutic paradigms in non-small cell lung carcinoma: high accuracy of tumor subtyping and feasibility of EGFR and KRAS molecular testing. J Thorac Oncol. 2011 Mar;6(3):451–8.

11 Edwards SL, Roberts C, McKean ME, Cockburn JS, Jeffrey RR, Kerr KM. Preoperative histological classification of primary lung cancer: accuracy of diagnosis and use of the non-small cell category. J Clin Pathol. 2000 Jul;53(7):537–40.

12 Nizzoli R, Tiseo M, Gelsomino F, Bartolotti M, Majori M, Ferrari L, et al. Accuracy of fine needle aspiration cytology in the pathological typing of non-small cell lung cancer. J Thorac Oncol. 2011 Mar;6(3):489–93.

13 Johnston WW, Frable WJ. The cytopathology of the respiratory tract. A review. Am J Pathol. 1976 Aug;84(2):372–424.

14 Nandeesh B, Crasta J, Tirumalae R. Fine-needle aspiration cytology in the diagnosis and typing of lung carcinomas. Clin Cancer Investig J. 2015 Sep 1;4(5):637–44.

15 MacDonald LL, Yazdi HM. Fine-needle aspiration biopsy of bronchioloalveolar carcinoma. Cancer. 2001 Feb 25;93(1):29–34.

16 Morency E, Rodriguez Urrego PA, Szporn AH, Beth Beasley M, Chen H. The "drunken honeycomb" feature of pulmonary mucinous adenocarcinoma: a diagnostic pitfall of bronchial brushing cytology. Diagn Cytopathol. 2013 Jan;41(1):63–6.

17 Idowu MO, Powers CN. Lung cancer cytology: potential pitfalls and mimics - a review. Int J Clin Exp Pathol. 2010 Mar 25;3(4):367–85.

Figure Legends

Fig. 1.

Diagnostic procedure of biopsies and surgical specimens. NSCLC, non-small cell lung carcinoma; IHC, immunohistochemistry; ADC, adenocarcinoma; SQCC, squamous cell carcinoma.

Fig. 2.

Adenocarcinoma case showing the isolated cell feature. Poorly cohesive singly scattered tumor cells are seen.

Fig. 3.

Adenocarcinoma case showing the flat sheet feature. The cluster is composed of mono-layered tumor cells.

Fig. 4.

Adenocarcinoma case showing three-dimensional clusters with irregular arrangement. The cluster is composed of multilayer tumor cells with irregular arrangement.

Fig. 5.

Adenocarcinoma case showing papillary-like structures. Peripheral cells of the cluster protrude outward in peninsula shape. There is no fibrovascular core in this case.

Fig. 6.

Adenocarcinoma case showing micropapillary-like structures. The clusters are composed of 3–20 tumor cells. They show flower crown-like, ball-like, or mulberry-like formation.

Fig. 7.

Adenocarcinoma case showing acinar-like structures. There is a circular arrangement of cells with lacuna in the cluster (arrow).

Fig. 8.

Adenocarcinoma case showing a palisading patterns. At the periphery of the cluster, the columnar cells show a palisading pattern (arrow).

Fig. 9.

Adenocarcinoma case showing protrusion of nuclei at the periphery of the cluster. At the periphery of the cluster, some nuclei protrude outward (arrow).

Fig. 10.

Adenocarcinoma case showing a honeycomb pattern. The cluster is composed of mono-layered tumor cells. The cell borders are relatively clear.

Fig. 11.

Squamous cell carcinoma case showing streaming arrangements and flattening at the periphery of the cluster. Tumor cells with oval or spindle nuclei present fascicular structure in the cluster. Elongated and flat nuclei are seen at the periphery of the cluster (arrow).

Fig. 12.

Squamous cell carcinoma case showing three-dimensional sheets with regular arrangement. The cluster is composed of multilayered tumor cells with relatively evenly spaced nuclei.

Fig. 13.

Squamous cell carcinoma case showing fuzzy patterns at the periphery of the cluster. Cytoplasmic elongation toward the outside of the cluster is seen (arrow).

Fig. 14.

Squamous cell carcinoma case showing the mutual inclusion feature. One tumor cell pushes another tumor cell as if englobing it (arrow).

Table 1. Sensitivity, specificity, positive predictive value, negative predictive value, and *p* value of each cytological structural feature

Cytological structural feature	Histological type		SE	SP	PPV	NPV	*p* value
	ADC (n = 149)	SQCC (n = 84)					
Isolated cell	137	78	91.9	7.1	63.7	33.3	0.803
Flat sheet	42	5	28.2	94.0	89.4	42.5	< 0.001
Three-dimensional cluster with irregular arrangement	137	76	91.9	9.5	64.3	40.0	0.701
Papillary-like structure	64	11	43.0	86.9	85.3	46.2	< 0.001
Micropapillary-like structure	9	0	6.0	100.0	100.0	37.5	0.028
Acinar-like structure	52	5	35.1	94.0	91.2	45.1	< 0.001
Palisading pattern	4	1	2.7	80.0	98.8	36.4	0.656
Protrusion of nuclei at the periphery of the cluster	122	35	81.9	58.3	77.7	64.5	< 0.001
Honeycomb pattern	2	0	1.3	100.0	100.0	36.4	0.537
Streaming arrangement	11	47	56.0	92.6	81.0	78.9	< 0.001
Three-dimensional sheets with regular arrangement	3	34	40.5	98.0	91.9	74.5	< 0.001
Flattening at the periphery of the cluster	17	50	59.5	88.6	74.6	79.5	< 0.001
Fuzzy pattern at the periphery of the cluster	12	24	28.6	91.9	66.7	69.5	< 0.001
Mutual inclusion	38	61	72.6	74.5	61.6	82.8	< 0.001

ADC, adenocarcinoma; SQCC, squamous cell carcinoma; SE, sensitivity; SP, specificity; PPV, positive predictive value; NPV, negative predictive value

Fig. 1

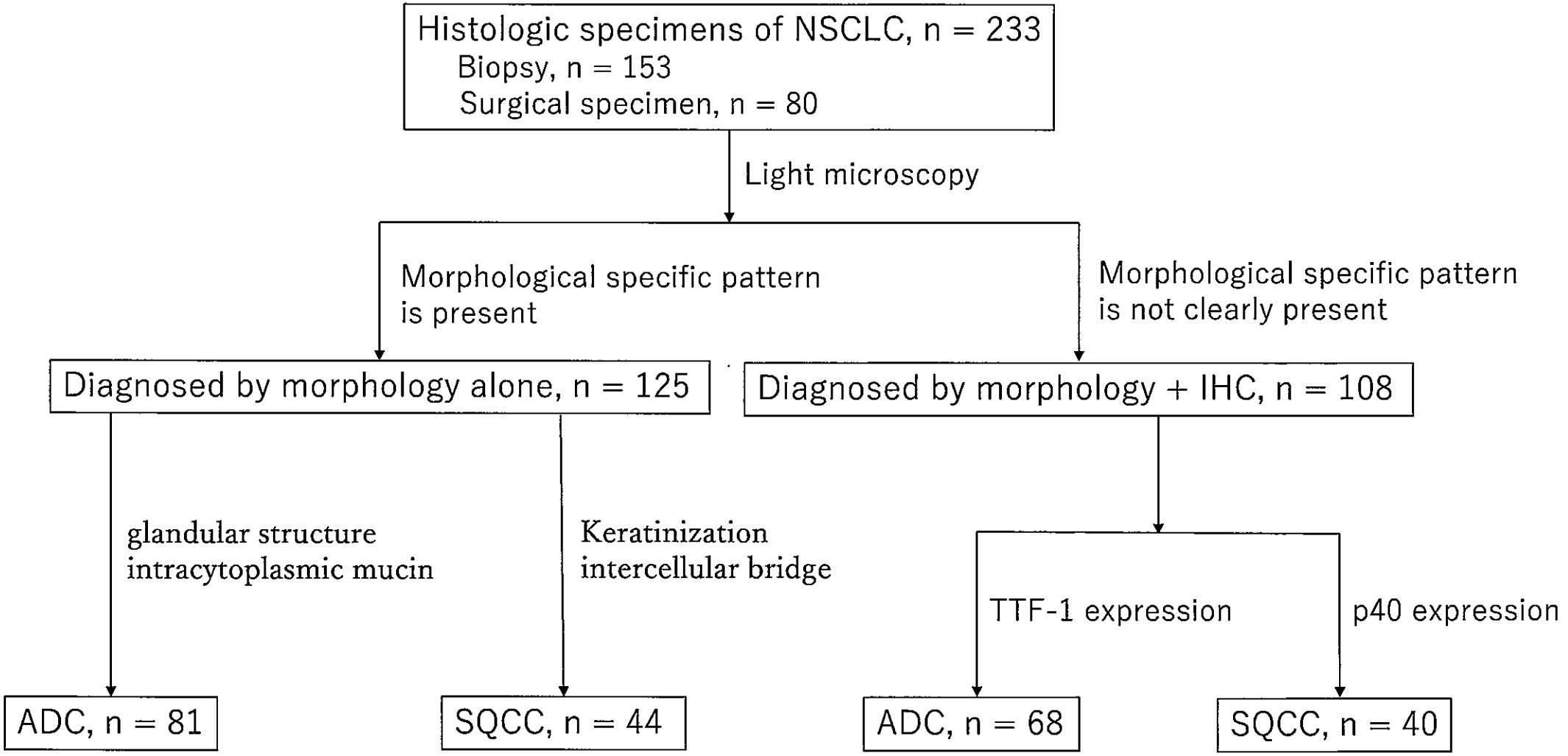
Histologic specimens of NSCLC, n = 233
Biopsy, n = 153
Surgical specimen, n = 80
Light microscopy
Morphological specific pattern is present
Morphological specific pattern is not clearly present
Diagnosed by morphology alone, n = 125
Diagnosed by morphology + IHC, n = 108
glandular structure
intracytoplasmic mucin
Keratinization
intercellular bridge
TTF-1 expression
p40 expression
ADC, n = 81
SQCC, n = 44
ADC, n = 68
SQCC, n = 40

Fig. 2

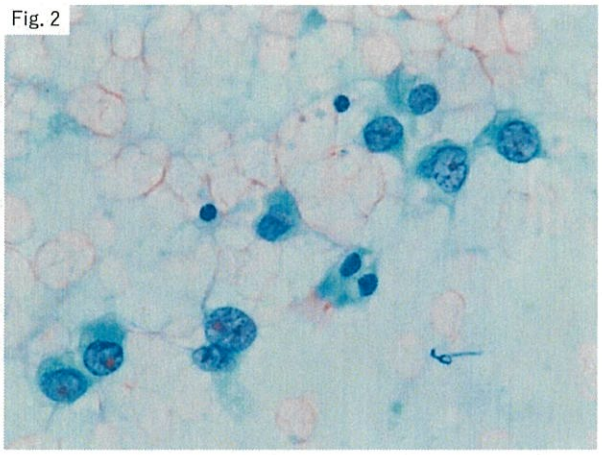

Fig. 3

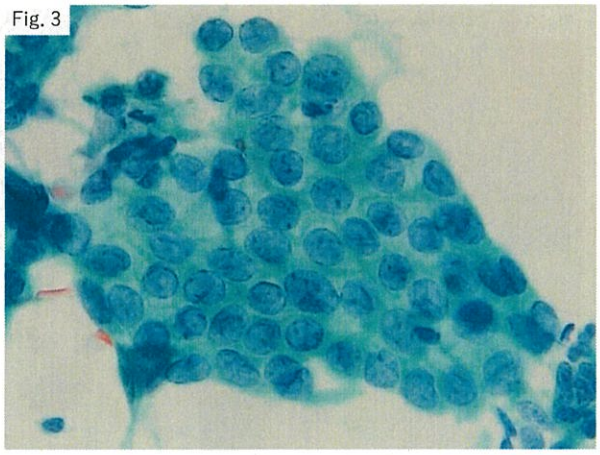

Fig. 4

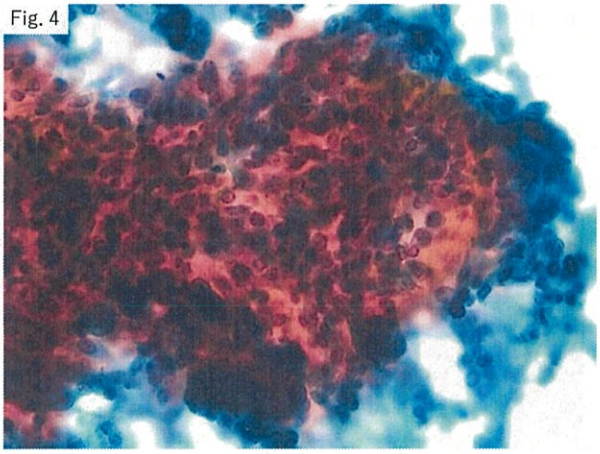

Fig. 5

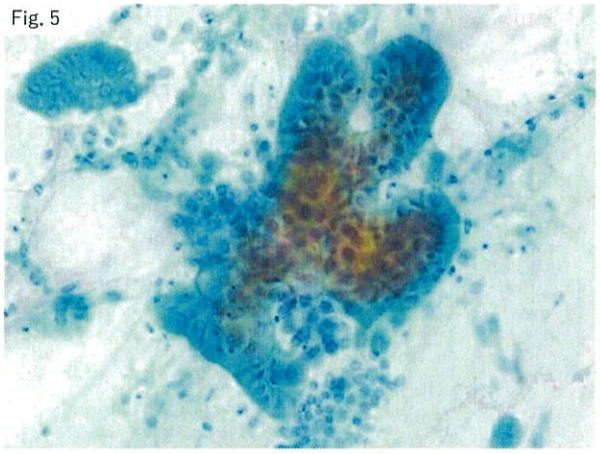

Fig. 6

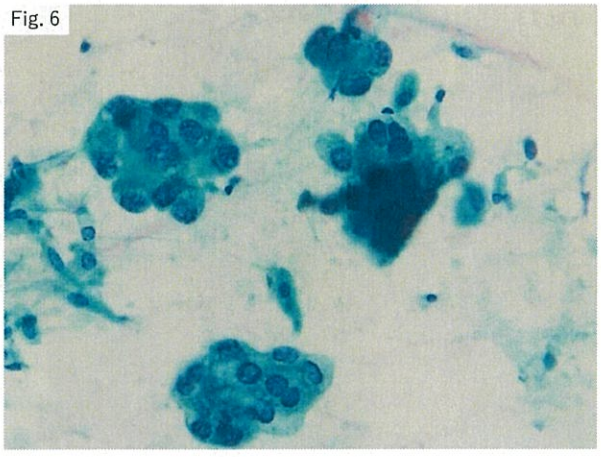

Fig. 7

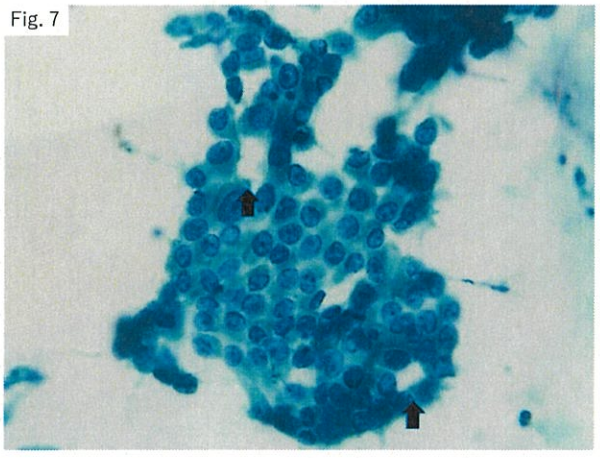

Fig. 8

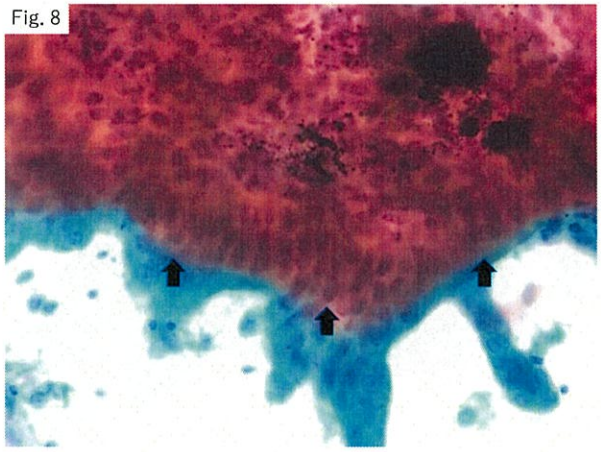

Fig. 9

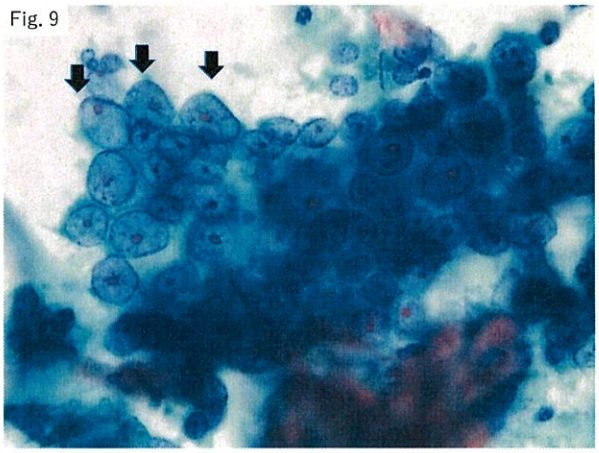

Fig. 10

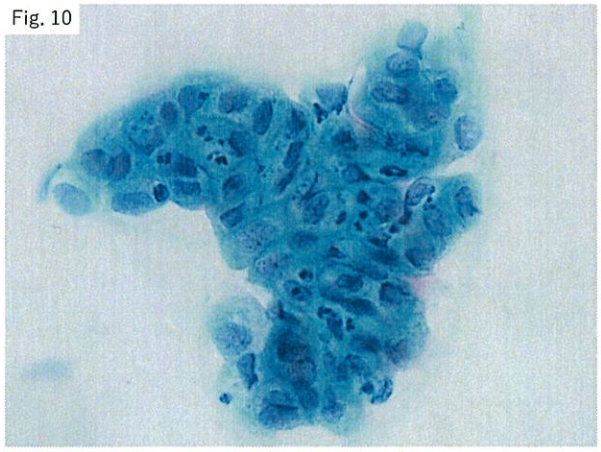

Fig. 11

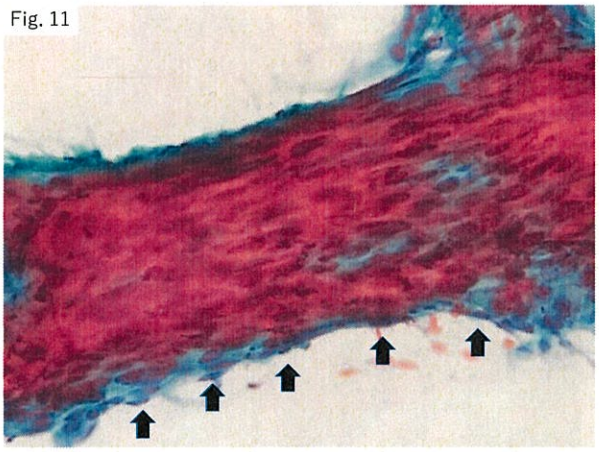

Fig. 12

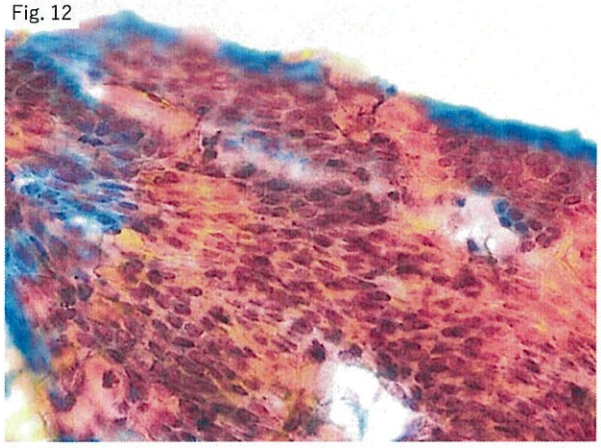

Fig. 13

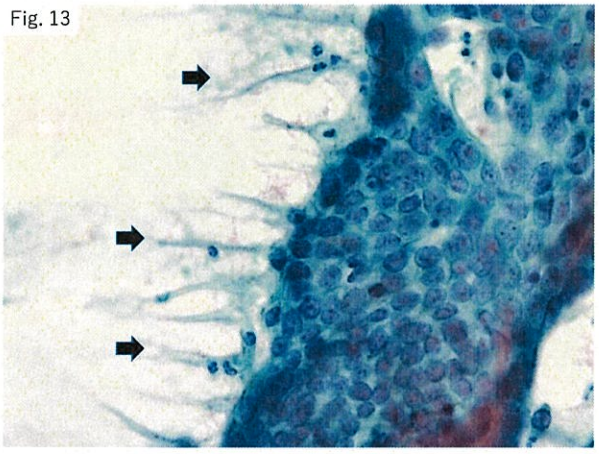

Fig. 14